

Solution Processed Tungsten Oxide Interfacial Layer for Efficient Hole-Injection in Quantum Dot Light-Emitting Diodes

Xuyong Yang, Evren Mutlugun, Yongbiao Zhao, Yuan Gao, Kheng Swee Leck, Yanyan Ma, Lin Ke, Swee Tiam Tan, Hilmi Volkan Demir,* and Xiao Wei Sun*

Light-emitting diodes (LEDs) based on colloidal quantum dots (QDs) are highly promising for the next generation of lighting and displays thanks to their narrow emission linewidth,^[1–4] tunable color emission spectral window across the visible to near-infrared range,^[5–7] and cost-effective fabrication techniques compatible with solution processed methods.^[8–12] Ever since the first demonstration of QD-based LEDs (QLEDs) 18 years ago,^[13] rapid progress has been made in the device performances owing to the technological development and accumulation of relevant knowledge in materials and device architectures, i.e., understanding the underlying device physics,^[14–16] designing more efficient

device architectures,^[17–20] and improving quantum dot properties by adjusting their composition and structure.^[21–23] To date, QLEDs have emerged as an undeniable competitor to organic light-emitting diodes (OLEDs) for lighting and display applications. However, despite their apparent advantages, long-term stability of QLEDs is still a big concern for their practical applications.

Traditionally, polyethylene dioxythiophene:polystyrene sulfonate (PEDOT:PSS) is the most widely used buffer layer on an indium tin oxide (ITO) electrode for the fabrication of QLEDs. However, the aqueous PEDOT:PSS dispersion causes a side effect on the QLED stability due to its hygroscopic nature as well as acidic nature corroding the ITO electrode, resulting in the reduction of device lifetime.^[24,25] Furthermore, compared with the inorganic material-based devices, the organic interfacial buffer layers have inferior thermal stability. Efforts to replace PEDOT:PSS with metal-oxides such as tungsten-, molybdenum-, nickel-, copper (I)-, rhenium-, or vanadium-oxides (WO_3 , MoO_3 , NiO , Cu_2O , ReO_3 , or V_2O_5) have gained significant importance in the recent years.^[26–31] In particular, highly n-doped WO_3 and MoO_3 exhibiting remarkably deep lying electronic states and efficient hole-injection into organic materials have been demonstrated.^[32–35] However, their unique electronic properties have so far been primarily achieved using thin films made by high-cost thermal evaporation under vacuum, which presents disadvantages due to the cost issues and incompatibility with roll-to-roll scalable manufacturing. Additionally, it has been demonstrated that metal-oxide nanoparticles (NPs) as the interfacial buffer layers are often more efficient as compared to their bulk counterparts. For example, ZnO nanoparticle films as the electron transporting layers (ETLs) prepared by a sol-gel method have been introduced, resulting in all-solution-processed QLEDs with the maximum brightness values of $31\,000\text{ cd m}^{-2}$, $68\,000\text{ cd m}^{-2}$ and 4200 cd m^{-2} for red, green and blue devices, respectively, which are among the highest reported thus far.^[8] Recently, Meyer's group reported the preparation of solution-processed MoO_3 nanoparticle films where the MoO_3 was spin-coated on ITO from a suspension containing MoO_3 nanoparticles and a block copolymer dispersing agent in xylene.^[36] However, the films require an extra O_2 -plasma treatment to remove the polymeric dispersing agent to facilitate hole injection in the device and the

X. Y. Yang, Dr. E. Mutlugun, Dr. Y. B. Zhao, K. S. Leck, Dr. S. T. Tan, Prof. H. V. Demir, Prof. X. W. Sun
Luminous! Center of Excellence for Semiconductor Lighting and Displays,
School of Electrical and Electronic Engineering
Nanyang Technological University
Nanyang Avenue, Singapore, 639798, Singapore
E-mail: hvdemir@ntu.edu.sg; EXWSun@ntu.edu.sg



Dr. E. Mutlugun, Prof. H. V. Demir
Department of Electrical and Electronics Engineering
Department of Physics, UNAM – Institute of Materials Science and Nanotechnology,
Bilkent University
Bilkent, Ankara, 06800, Turkey

Y. Gao, Prof. H. V. Demir
School of Physical and Mathematical Sciences
Nanyang Technological University
Nanyang Avenue, Singapore, 639798, Singapore

Y. Y. Ma
State Key Lab of Luminescence Materials and Devices
Institute of Optical Communication Materials
South China University of Technology
Guangdong, 510641, China

Dr. L. Ke
Institute of Materials Research and Engineering
A* STAR (Agency for Science, Technology and Research)
3 Research Link, Singapore, 117602, Singapore
Prof. X. W. Sun
South University of Science and Technology
1088 Xue-Yuan Road, Shenzhen, Guangdong, 518055, China.

DOI: 10.1002/sml.201301199

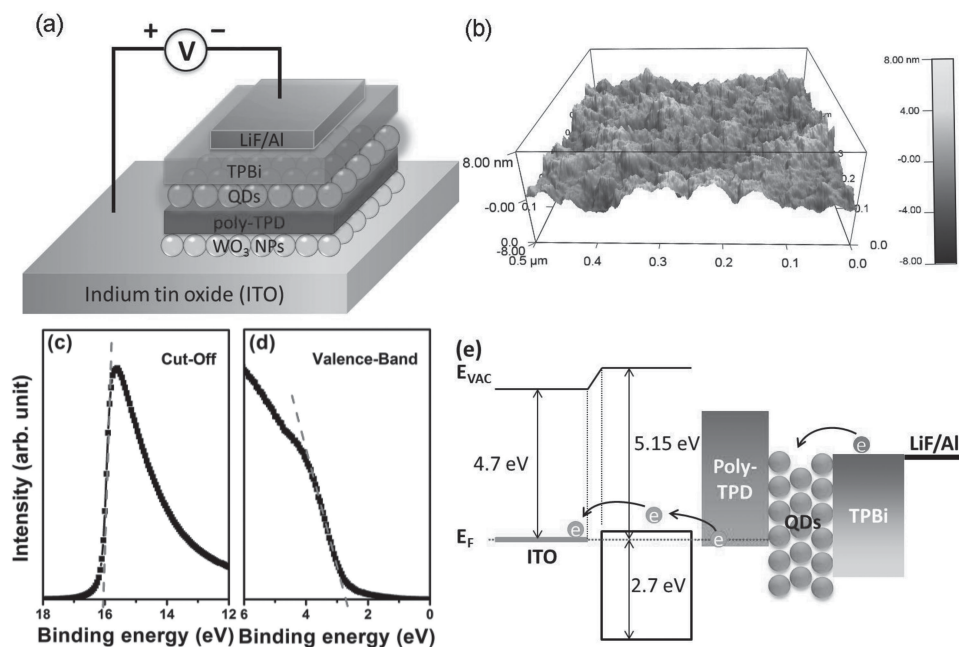


Figure 1. (a) Schematic of the device configuration of the QLEDs. (b) AFM image of WO_3 nanoparticle HTL formed on ITO substrate. UPS spectra of a WO_3 nanoparticle film annealed at 100°C including (c) secondary-electron cutoff and (d) zoom-in section of the evolution of the density of states near the oxide valence band edge. (e) Energy level diagram of the WO_3 nanoparticle-based QLEDs.

resulting surface of MoO_3 nanoparticle film was relatively rough. Therefore, as such, in-depth studies focusing on solution-processed inorganic interfacial buffer layers is of critical importance for improving the QLED performance.

Here we report a highly efficient, stable QLED using solution-processed WO_3 nanoparticles as the hole injection layer. The preparation of the WO_3 nanoparticle layer described here is simple and cost-effective employing cheap and commercially available WO_3 nanoparticles and ethanol as a solvent and utilizing a low-temperature process under ambient conditions (annealing temperature can be as low as 80°C and without requiring the O_2 -plasma treatment). This treatment temperature is much lower than that of PEDOT:PSS (120 – 150°C). At the same time, the overall performance for WO_3 nanoparticle-based QLED is superior compared to that of the present PEDOT:PSS-based QLEDs using the same device architecture. The WO_3 nanoparticle-based QLEDs with a maximum brightness of $30,006\text{ cd/m}^2$, an external quantum efficiency (EQE) of 3.32%, and a peak current efficiency of 10.75 cd A^{-1} have been achieved. Besides, the device lifetime has been also improved remarkably compared to that of PEDOT:PSS-based QLEDs, which marks as a further step towards the practical application of the QLED technology.

The standard structure of QLEDs is given as a multilayer structure of ITO/poly(3,4-ethylenedioxythiophene)poly(styrenesulfonate)(PEDOT:PSS)/Poly[*N,N'*-bis(4-butylphenyl)-*N,N'*-bis(phenyl)benzidine] (poly-TPD)/QDs/2, 2', 2''-(1, 3, 5-benzinetriyl)-tris(1-phenyl-1-*H*-benzimidazole) (TPBi)/LiF/Al.^[17,22] The CdSe/ZnS core-shell structured QDs prepared according to a previous reported literature were used for the emissive layer.^[3] The poly-TPD and TPBi layers were chosen as the hole transport layer (HTL) and the electron transport layer (ETL), respectively.

In our case, the WO_3 nanoparticle layer spin-coated on ITO was used to replace PEDOT:PSS as the HIL. The device structure is schematically presented in **Figure 1a**. The atomic force microscopy (AFM) image of the close-packed thin film of WO_3 nanoparticles on ITO with an average particle size of 7 nm (annealed at 100°C in the glove box) is shown in Figure 1b. The surface roughness (RMS) of the film made from a 2 wt% of WO_3 ethanol solution is only 2.8 nm, indicating that the nanoparticle film has a smooth surface. To confirm the electronic structure of the as-prepared WO_3 nanoparticle film, the ultraviolet photoelectron spectroscopy (UPS) spectra including the magnified regions of the photoemission cut-off and valence band are given in Figures 1c and 1d. The photoemission onset is found at 16.05 eV from the photoemission cut-off in Figure 1c. This corresponds to a work function (WF) of 5.15 eV in agreement with the WF values of WO_3 reported in literature, which can range from 4.7 to 6.4 eV depending on the film preparation conditions.^[37] Figure 1d displays the zoom-in spectra of the density of states near the oxide valence band edge and the ionization energy (IE) of the WO_3 film that is determined to be 2.7 eV with respect to the Fermi level. According to the schematic energy level diagram of the device depicted in Figure 1e, it can be observed that the electrons can easily be injected from the Al to the QD layer. However, the case is quite different for the hole injection.^[24,34,36] Owing to the deep lying electronic states of WO_3 nanoparticle interface layer, efficient hole injection can be proceeded via electron extraction from the highest occupied molecular orbital (HOMO) level of poly-TPD into the conduction band of WO_3 nanoparticles. For n-doped WO_3 or MoO_3 , the hole injection from ITO to the organic semiconductors results from electron extraction from the highest occupied molecular orbital (HOMO) level

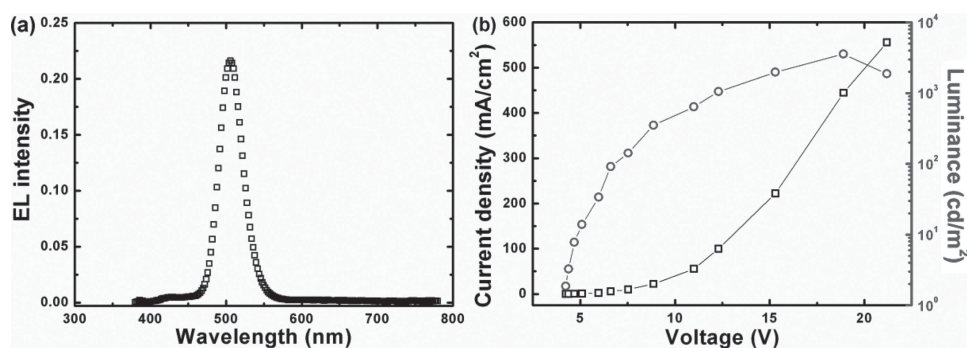


Figure 2. (a) EL spectrum and (b) current density-voltage and luminance-voltage characteristics of QLED.

of organic semiconductors through the WO_3 or MoO_3 conduction band, and then into ITO. For our case, owing to the deep lying electronic states of WO_3 nanoparticle interface layer, the energy barrier for the injection of electrons from the HOMO level of to the conduction band of WO_3 nanoparticles is quite small, and the efficient hole injection can be proceeded via electron extraction from the HOMO level of poly-TPD into the conduction band of WO_3 nanoparticles.

Figure 2a presents the output performance of an optimized WO_3 nanoparticle-based QLED. The device is fabricated with QDs of 4 monolayers-equivalent thickness (~20 nm) and a WO_3 nanoparticle film of 2 monolayers-equivalent thickness (~14 nm). The electroluminescence (EL) spectrum of the QLED was recorded at the bias voltage of 12 V, showing a characteristic QD EL peak centered at ~518 nm with a full-width-at-half-maximum (FWHM) of ~30 nm. It should be noted here that there is a weak emission in the blue-wavelength region due to the residual emission from poly-TPD. The emission from poly-TPD indicates the possible imbalance of the charge in the QD layer. The electrons on the lowest unoccupied molecular orbital (LUMO) of TPBi can jump over the 0.9 eV energy barrier into the LUMO of poly-TPD through defects of the QD layer to combine with holes in the poly-TPD layer. This phenomenon can be observed in almost all PEDOT:PSS-based QLEDs. **Figure 2b** shows the luminance and current density characteristics of the device as a function of the applied voltage. The luminance-current density-voltage characteristics show a low turn-on voltage of 3.6 V and a peak luminance of 3565 cd/m^2 at a current density of 444.44 mA/cm^2 . The maximum EQE of 0.43% was obtained under the same current density.

To further improve the performance of WO_3 nanoparticle-based QLEDs, we deposited a 2,2',2''-tris-(N-carbazolyl)-triphenylamine (TCTA) electron-blocking layer (EBL) on the QD layer to suppress the excess electrons for improving the charge balance of device. The LUMO of TCTA is 2.4 eV^[38] and the relatively high energy barrier of 0.8 eV between the LUMO of TCTA and that of TPBi can block electrons to reach the poly-TPD layer in the device effectively. **Figure 3a** shows the EL spectra for the device with TCTA utilized as the EBL under different driving currents. It can be observed that the blue emission of poly-TPD is hardly found even in the case of a high driving current, as electrons from TPBi are completely blocked by the TCTA EBL before jumping into

the LUMO of poly-TPD. This is another advantage of using TCTA because the blue emission from poly-TPD degrades the color purity. Compared with the original QLEDs without the TCTA used as the EBL, the performance of QLED with TCTA is increased significantly, showing the maximum luminance, EQE and current efficiency values of 30 006 cd m^{-2} and 3.32%, respectively. To the best of our knowledge, the EQE of 3.32% is much higher than the previously reported values for green QLEDs with normal architecture (the recently reported green QLEDs using the inverted architecture reached an EQE level of 5.8%).^[17] A corresponding image of the QLED output was recorded at the luminance of 300 cd/m^2 , which displays bright and saturated green emission (**Figure 3b**). **Figures 3c** and **3d** show a comparison of the luminance-current density ($L-J$) and efficiency-current density ($E-J$) characteristics of the WO_3 nanoparticle-based QLED and an optimized PEDOT:PSS-based QLED with the same structure. As can be seen, the two devices show a similar trend in the $L-J$ and $E-J$ characteristics, as the driving current is increased. **Table 1** summarizes the key figures of the two QLEDs. The maximum brightness, EQE, current efficiency and efficacy for the WO_3 nanoparticle-based QLED are superior. Also, the turn-on voltage of the WO_3 nanoparticle-based QLED decreases to 3.8 V, which is lower than that observed for the PEDOT:PSS-based device (4.2 V). Moreover, it can be noted that the WO_3 nanoparticle-based QLED still works well even under the current of 50 mA, while the PEDOT:PSS-based QLED has burned down when the driving current is just 40 mA, which indicates the better device stability for the WO_3 nanoparticle-based QLED.

Figure 4 shows the operating stability of the resulting unencapsulated WO_3 nanoparticle-based QLED in comparison with the optimized PEDOT:PSS-based QLED. Under a continuous current driving condition corresponding to an initial luminance of 1000 cd/m^2 , it can be clearly observed that using WO_3 nanoparticles to replace PEDOT:PSS as the HILs in QLEDs can drastically improve device stability. The unencapsulated WO_3 nanoparticle-based QLED displays a half-lifetime of ca. 6530 s, showing an approximately two-fold lifetime enhancement as compared to that of PEDOT:PSS-based QLED. The significant improvement in the device stability can be attributed to the fact that WO_3 nanoparticles are highly stable when compared to organic materials and can therefore act as a protection layer for organic materials.

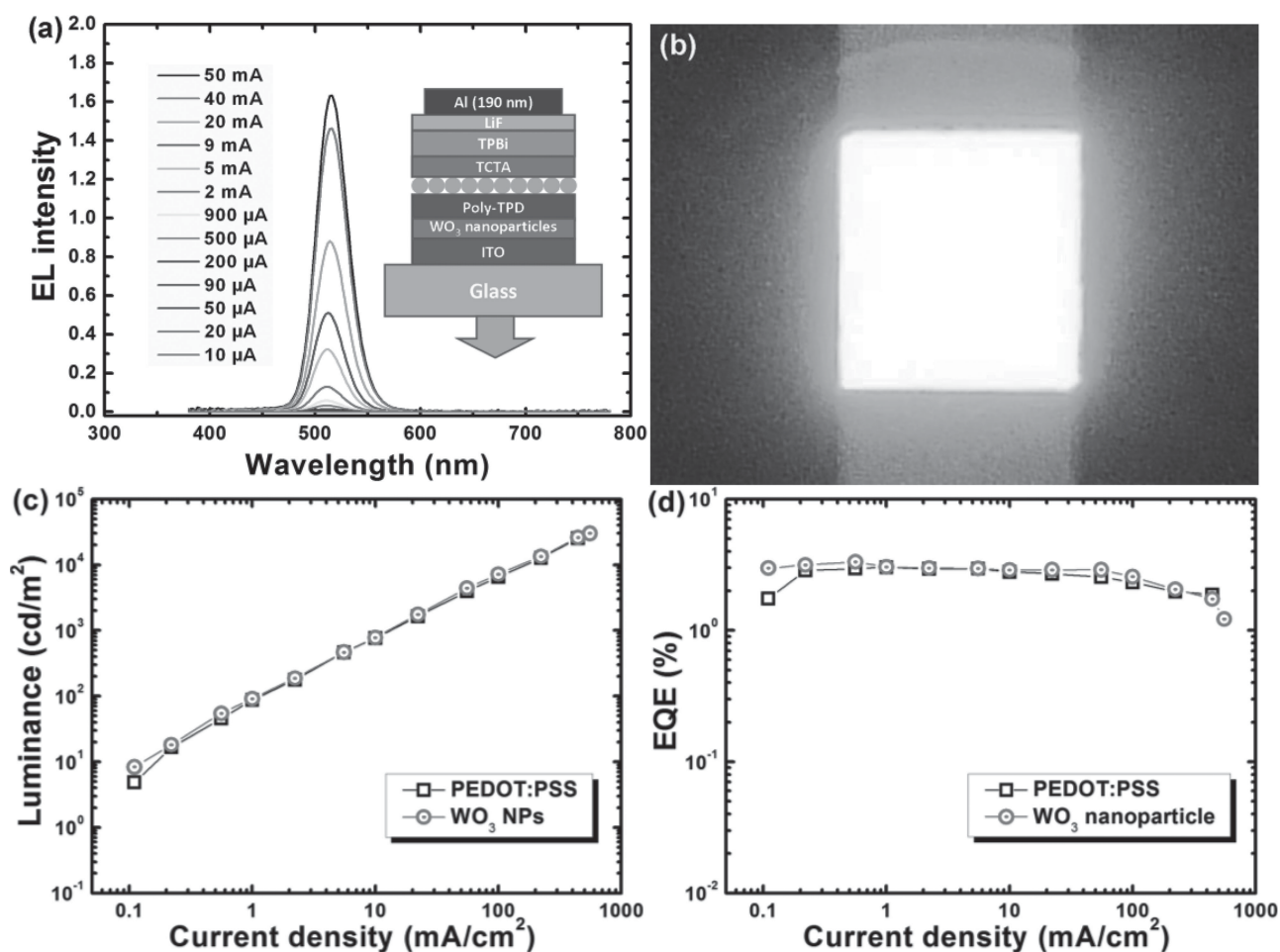


Figure 3. (a) EL spectra of the device at different injection currents (inset shows the schematic cross section of the device structure used in this study). (b) The photograph of a QLED under operation with a pixel size of 3 mm×3 mm. (c) Luminance (cd m^{-2}) and (d) external quantum efficiency (%) of QLEDs using PEDOT:PSS and WO_3 nanoparticles as the HTLs as a function of current density (mA cm^{-2}).

In summary, we have demonstrated an efficient QLED using solution-processed WO_3 nanoparticle film instead of using PEDOT:PSS as the anode interfacial buffer layer. The WO_3 nanoparticle-based QLEDs show enhanced performance as compared to the PEDOT:PSS-based QLEDs. The EQE of 3.32% reported here is the highest value for green QLEDs using a non-inverted structure and the brightness of 30 006 cd/m^2 matches that of the best QLEDs with organic materials used as HTLs/HILs. Moreover, with the incorporation of the WO_3 nanoparticles, the unencapsulated device exhibits a significant improvement in the device stability and the lifetime is increased by approximately two-folds at

an initial brightness of 1000 cd/m^2 as compared to that of PEDOT:PSS-based QLED. Meanwhile, since the solution-processed preparation method of WO_3 nanoparticle film used in our work is very simple and can be achieved at low annealing temperatures, it is suitable for application in flexible devices where the flexible substrates such as plastics often cannot withstand high annealing temperatures. These results indicate that WO_3 nanoparticles are promising solution-processed buffer layer materials and offer a practicable platform for the realization of high-performance, stable and large-area commercial QLEDs using a low-cost manufacturing process.

Table 1. List of figure-of-merits to compare the device performance using WO_3 nanoparticles (A) and PEDOT:PSS (B) as HILs.

Device	$V_{\text{turn-on}}$ [V]	Max. Luminance [cd/m^2]	Max. EQE [%]	Max. Current efficiency [cd/A]	Max. Efficacy [lm/W]	Lifetime [s]
A	3.8	30 006 (@50 mA)	3.32	9.75	6.8	6530
B	4.2	25 202 (@40 mA)	3.02	8.74	6.0	3130

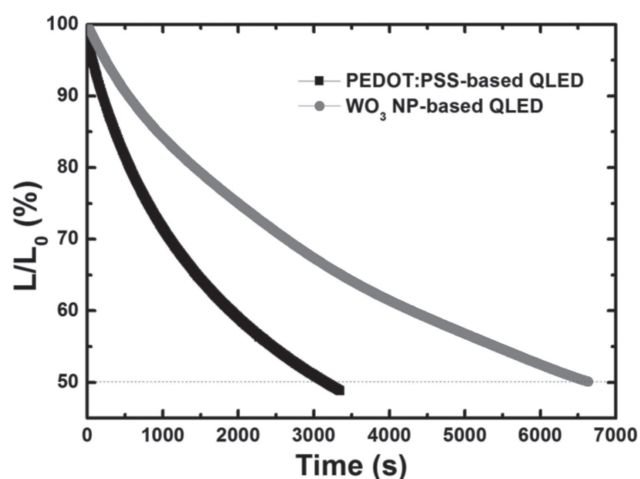


Figure 4. Operational lifetime characteristics of the resulting WO₃ nanoparticle based QLED and the optimized PEDOT:PSS based QLED. The luminance of these QLEDs was measured without using encapsulation and during the continuous operation at a constant current density corresponding to an initial luminance of 1000 cd/m². Both types of QLEDs were fabricated using the same device architecture.

Experimental Details

Synthesis of CdSe-ZnS Core-Shell QDs: Green-emitting CdSe-ZnS QDs with a chemical-composition gradient were prepared according to a modified method reported in the literature.^[3] For a typical preparation of green-emitting QDs, 0.1 mmol of cadmium oxide (CdO), 4 mmol of zinc acetate (Zn(AcEt)₂), 5 mL of oleic acid (OA) were loaded in a 50 mL 3-neck flask, heated to 150 °C under vacuum to form cadmium oleate (Cd(OA)₂) and zinc oleate (Zn(OA)₂). Then 20 mL of 1-octadecene (1-ODE) was added to the reaction flask and the reactor was then filled with nitrogen and heated up to 300 °C. At the elevated temperature, 1.6 mL of tri-n-octylphosphine (TOP) dissolving 0.15 mmol of selenium (Se) and 4 mmol of sulphur (S) was injected into the flask swiftly, and the reaction mixture were maintained at 300 °C for 10 min for the QD growth. To purify the synthesized QDs, the reaction mixture was cooled down to room temperature, and the QDs were extracted by the addition of acetone and methanol, followed by centrifugation. The CdSe-ZnS core-shell QDs were readily dispersed in toluene.

Fabrication of QLED Devices: The patterned ITO substrates were cleaned by sonication sequentially in detergent, de-ionized water, acetone, and isopropyl alcohol. The WO₃ anode buffer layer was spin-coated on the O₂-plasma treated ITO substrate from diluted 1.25 wt% of WO₃ ethanol solution at 5000 rpm for 60 s and annealed at 80–110 °C for 30 min. The 2 wt% of poly-TPD (50 nm) in chlorobenzene was also spin-coated on the WO₃ layer at 4000 rpm for 60 s, followed by thermal annealing at 150 °C for 30 min in a nitrogen glove box. The QD layer was then deposited on the ITO/WO₃/poly-TPD layer by spin-coating the QD dispersion (QDs were dispersed in toluene with 15 mg/mL) at a rate of 1000–4000 rpm for 60 s, and cured at 90 °C under N₂ atmosphere for 30 min. The TPBi (35 nm), LiF (0.5 nm), and Al (190 nm) layers were thermally deposited under a base pressure of ~2 × 10⁻⁴ Pa. WO₃ dispersion in ethanol (2.5 wt%) was purchased from Nano-grade GmbH (product no. 4035). For PEDOT:PSS based QLEDs, we

followed the same procedure and only the WO₃ layer was replaced by PEDOT:PSS layer (40 nm) which was spun on the ITO substrate at 4000 rpm for 60 s and annealed at 150 °C for 30 min.

Instrumentation: AFM (Cypher AFM, Asylum Research) was used to image the WO₃ nanoparticle film. UPS was performed using X-Ray Photoelectron spectroscopy (XPS) (VG Escalab 220i XL) with a He I (21.2 eV) gas discharge lamp. The electroluminescence (EL) spectra of the fabricated devices were measured using a PR650 Spectra Scan spectrometer, while the luminance-current density-voltage (L-J-V) characteristics were obtained simultaneously, by connecting the spectrometer to a programmable Keithley 236 source measurement unit. All measurements were carried out at room temperature under ambient conditions.

Acknowledgments

The authors would like to thank the financial support from Singapore National Research Foundation under NRF-RF-2009-09 and NRF-CRP-6-2010-02 and the Science and Engineering Research Council, Agency for Science, Technology and Research (A*STAR) of Singapore (project Nos. 092 101 0057 and 112 120 2009). The work is also supported by the National Natural Science Foundation of China (NSFC) (project Nos. 61006037 and 61076015).

- [1] Y. Shirasaki, G. J. Supran, M. G. Bawendi, V. Bulović, *Nat. Photonics* **2013**, *7*, 13–23.
- [2] K. S. Cho, E. K. Lee, W. J. Joo, E. Jang, T. H. Kim, S. J. Lee, S. J. Kwon, J. Y. Han, B. K. Kim, B. L. Choi, J. M. Kim, *Nat. Photonics* **2009**, *3*, 341–345.
- [3] W. K. Bae, J. Kwak, J. Lim, D. Lee, M. K. Nam, K. Char, C. Lee, S. Lee, *Nano Lett.* **2010**, *10*, 2368–2373.
- [4] V. Wood, V. Bulović, *Nano Rev.* **2010**, *1*, 5202–5208.
- [5] X. Yang, D. Zhao, K. S. Leck, S. T. Tan, Y. X. Tang, J. Zhao, H. V. Demir, X. W. Sun, *Adv. Mater.* **2012**, *24*, 4180–4185.
- [6] P. O. Anikeeva, J. E. Halpert, M. G. Bawendi, V. Bulović, *Nano Lett.* **2009**, *9*, 2532–2536.
- [7] L. Sun, J. J. Choi, D. Stachnik, A. C. Bartnik, B.-R. Hyun, G. G. Malliaras, T. Hanrath, F. W. Wise, *Nat. Nanotechnol.* **2012**, *7*, 369–373.
- [8] L. Qian, Y. Zheng, J. Xue, P. H. Holloway, *Nat. Photonics* **2011**, *5*, 543–548.
- [9] Y. Zhang, C. Xie, H. Su, J. Liu, S. Pickering, Y. Wang, W. W. Yu, J. Wang, Y. Wang, J. I. Hahm, N. Dellas, S. E. Mohny, J. Xu, *Nano Lett.* **2011**, *11*, 329–332.
- [10] M. A. Schreuder, K. Xiao, I. N. Ivanov, S. M. Weiss, S. J. Rosenthal, *Nano Lett.* **2010**, *10*, 573–576.
- [11] Z. Tan, F. Zhang, T. Zhu, J. Xu, A. Y. Wang, J. D. Dixon, L. Li, Q. Zhang, S. E. Mohny, *Nano Lett.* **2007**, *7*, 3803–3807.
- [12] Z. Tan, Y. Zhang, C. Xie, H. Su, J. Liu, C. Zhang, N. Dellas, S. E. Mohny, Y. Wang, J. Wang, J. Xu, *Adv. Mater.* **2011**, *23*, 3553–3558.
- [13] V. L. Colvin, M. C. Schlamp, A. P. Alivisatos, *Nature* **1994**, *370*, 354–357.
- [14] D. Bozyigit, O. Yarema, V. Wood, *Adv. Funct. Mater.* **2013**, doi: 10.1002/adfm.201203191.
- [15] X. Yang, Y. Divayana, D. Zhao, K. S. Leck, F. Lu, S. T. Tan, A. P. Abiyasa, Y. Zhao, H. V. Demir, X. W. Sun, *Appl. Phys. Lett.* **2012**, *101*, 233110–233113.

- [16] M. L. Mastronardi, E. J. Henderson, D. P. Puzzo, Y. Chang, Z. B. Wang, M. G. Helander, J. Jeong, N. P. Kherani, Z. Lu, G. A. Ozin, *Small* **2012**, *12*, 3647–3654.
- [17] J. Kwak, W. K. Bae, D. Lee, I. Park, J. Lim, M. Park, H. Cho, H. Woo, D. Y. Yoon, K. Char, S. Lee, C. Lee, *Nano Lett.* **2012**, *12*, 2362–2366.
- [18] V. Wood, M. J. Panzer, J. M. Caruge, J. E. Halpert, M. G. Bawendi, V. Bulović, *Nano Lett.* **2010**, *10*, 24–29.
- [19] E. M. Likovich, R. Jaramillo, K. J. Russell, S. Ramanathan, V. Narayanamurti, *Adv. Mater.* **2011**, *23*, 4521–4525.
- [20] Q. Sun, G. Subramanyam, L. Dai, M. Check, A. Campbell, R. Naik, J. Grote, Y. Wang, *ACS Nano* **2009**, *3*, 737–743.
- [21] B. N. Pal, Y. Ghosh, S. Brovelli, R. Laocharoensuk, V. I. Klimov, J. A. Hollingsworth, H. Htoon, *Nano Lett.* **2012**, *12*, 331–336.
- [22] W. K. Bae, J. Kwak, J. W. Park, K. Char, C. Lee, S. Lee, *Adv. Mater.* **2009**, *21*, 1690–1694.
- [23] B. Chen, H. Zhong, W. Zhang, Z. Tan, Y. Li, C. Yu, T. Zhai, Y. Bando, S. Yang, B. Zou, *Adv. Fun. Mater.* **2012**, *22*, 2011–2088.
- [24] S. Murase, Y. Yang, *Adv. Mater.* **2012**, *24*, 2459–2462.
- [25] J. J. Jasieniak, J. Seifert, J. Jo, T. Mates, A. J. Heeger, *Adv. Funct. Mater.* **2012**, *22*, 2594–2605.
- [26] M. T. Greiner, M. G. Helander, W.-M. Tang, Z.-B. Wang, J. Qiu, Z.-H. Lu, *Nat. Mater.* **2012**, *11*, 76–81.
- [27] J. M. Caruge, J. E. Halpert, V. Wood, V. Bulović, M. G. Bawendi, *Nat. Photonics* **2008**, *2*, 247–250.
- [28] Z. Tan, L. Li, C. Cui, Y. Ding, Q. Xu, S. Li, D. Qian, Y. Li, *J. Phys. Chem. C* **2012**, *116*, 18626–18632.
- [29] H. M. Wei, H. B. Gong, L. Chen, M. Zi, B. Q. Cao, *J. Phys. Chem. C* **2012**, *116*, 10510–10515.
- [30] J. Meyer, K. Zilberberg, T. Ried, A. Kahn, *J. Appl. Phys.* **2011**, *110*, 033710–033714.
- [31] J.-H. Lee, D.-S. Leema, H.-J. Kim, J.-J. Kim, *Appl. Phys. Lett.* **2009**, *94*, 123306–123308.
- [32] M. Sessolo, H. J. Bolink, *Adv. Mater.* **2011**, *23*, 1829–1845.
- [33] R. Acharya, X. A. Cao, *Appl. Phys. Lett.* **2012**, *101*, 053306–053309.
- [34] M. Kröger, S. Hamwi, J. Meyer, T. Riedl, W. Kowalsky, A. Kahn, *Appl. Phys. Lett.* **2009**, *95*, 123301–123303.
- [35] Z. B. Wang, M. G. Helander, J. Qiu, D. P. Puzzo, M. T. Greiner, Z. M. Hudson, S. Wang, Z. W. Liu, Z. H. Lu, *Nat. Photonics* **2011**, *5*, 753–757.
- [36] J. Meyer, R. Khalandovsky, P. Görrn, A. Kahn, *Adv. Mater.* **2011**, *23*, 70–73.
- [37] S. Han, W. S. Shin, M. Seo, D. Gupta, S.-J. Moon, S. Yoo, *Org. Electron.* **2009**, *10*, 791–797.
- [38] J. Y. Lee, M.-S. Gong, S. Ryu, G.-k. Chang, H. J. Chang, *J. Appl. Phys.* **2008**, *103*, 054502–054505.

Received: April 19, 2013
Revised: May 27, 2013
Published online: